Applied GIS

ISSN: 1832-5505
Vol-7 Issue-02 MAY 2019

Battery Energy Storage System Control for Mitigating PV Penetration Impact on Primary Frequency Control and State-of-Charge Recovery by using Fuzzy logic controller

D.SHEKSHA VALI, ASSISTANT PROFESSOR, shaikshavali456@gmail.com
C.SUMA LATHA, ASSISTANT PROFESSOR, sumalathacherukuri@gmail.com
G.VAMSI KRISHNA, ASSISTANT PROFESSOR, kvamsi706@gmail.com
Department of Electrical & Electronics Engineering, Sri Venkateswara Institute of Technology, N.H 44, Hampapuram, Rapthadu, Anantapuramu, Andhra Pradesh 515722D

Abstract—
A decrease in system idleness, which affects the damping power of frameworks to manage vital recurrence control, is one effect of increasing PV penetration. The PV energy system is not like a wind turbine in that it cannot store motor energy, making it unable to provide under-recurrence support; furthermore, it may impose penalties for ignoring administrative requirements. Consequently, a new adaptive state-of-charge recuperation approach with a fuzzy logic controller is suggested for use in a droop type lead-lag controlled battery energy storage system (BESS). Flexible SOC recovery does not affect the maximum SOC for the typical business event, and the suggested adaptive SOC system regulates SOC based on the benefit of charging current. The efficacy of BESS in reducing the unfavourable inertial impact of PV and meeting mandatory grid requirements is shown by the replication findings.

I. INTRODUCTION

The use of practical, environmentally friendly energy sources has been steadily increasing over the last decade, and experts predict that this trend will continue. Current planning scenarios suggest that, under accelerated conditions, infinite limit development is expected to reach a further 30% (1150GW) of the current assessment (920GW) by 2022, while PV limit development is needed to reach 59.6% [1]. So, it is important to think about the dynamic impacts of PV in transmission networks, and we still haven't looked at PV's implications on overall framework recurrence control in detail. Overall system inactivity is reduced by replacing simultaneous generators with less/non-inertial and uncertain RES.

as a result, when encountering power irregularities, the framework would have fundamental challenges in providing a rapid response to recurrences. Serious problems with power system activity and control might arise from insufficient capacity for recurrent backup [2]. There are available quantities of distributions on recurrence movements associated with PV entry in the power system. The authors of the solidness focuses in [3]-[5] argued that the framework's recurrent movements are expanded by a reduction in idleness. Even more so, the authors of [5] shown that a greater PV entry causes emotional recurrence that strays from lattice operating norms, which might pleasantly weaken continuous burden. In order to maintain effective damping performance and damp out force framework movements caused by transient force asymmetry, the PV terminal receives a force swaying damper [6], a coordinated force regulator [7], and a distinct model flexible control process [9]. We suggest a hang type control [10], designed latency control [11], and a working point lower than most extreme force point (MPP) [12] to guide framework recurrence and direct PV power yield. The authors of a related study found that combining hang and inactivity control outperforms either discrete hang and dormancy control or the standard MPP following. For this over-recurrence recommendation to work, PV power yield must be cut in half. Furthermore, PV is unable to provide under-recurrence support due to the lack of pivoting masses, such as stored energy, in contrast to wind turbines, which may provide a certain amount of under/over recurrence guidance utilising their stored dynamic energy. Because NEM has a plan to penalise users that disobey ancillary services for frequency control.

needs, therefore the backup fuel supply should make sure recurrence management is inside administrative imperatives and avoid penalties with the enlarged PV entry. BESS has shown remarkable promise in providing critical recurring savings during crisis situations to maintain network requirements. Enhanced damping performance is provided by BESS and other auxiliary devices, especially shunt capacitors and ultra-capacitors. However, knowledge of BESS estimation and battery SOC was not

ISSN: 1832-5505
Vol-7 Issue-02 MAY 2019

welcomed in the test. In addition, the near-term study only takes a 1% PV entry level into account, which downplays the gravity of the increased large-scale PV penetration. An isolated Microgrid and little force framework demonstrate the use of BESS in reducing vital recurrence. However, no renewable energy sources (RES) are included in the framework, and the study only covers small-scale power systems. For recurrence control and wavering damping, a lead-slack based BESS control is used; however, no SOC recovery approach was taken into account in the tests. Most of the studies have not suggested any ways to restore battery SOC. In their presentation, the authors highlighted how the SOC recovery method reduces guideline dissatisfaction and, thus, the accumulated penalty cost. The microgrid now has battery/super capacitor SOC recovery, which has been tested and approved. However, this does not make the most efficient use of the available battery limit as SOC recovery is restored to its apparent value. As a result of this shortfall, a portable SOC recovery is implemented; nonetheless, this method reduces the usually usable battery limit since the developers intended to limit the maximum and minimum SOC working area as part of their received approach. Using 18.18% PV entrance and a novel SOC recovery technique, this paper proposes a hang-type and lead-slack controlled BESS that can participate in essential recurrence control according to NEM framework requirements. It also aims to avoid recurrence infringement during possibility periods to avoid punishment from the transmission/dissemination framework administrator. Energy trading during critical recurrence control also has the potential to reduce battery SOC, even when it does not exceed the SOC limit. Consequently, aside than the conventional highest charging SOC limit, another

presentation of the suggested hang-controlled BESS, selection of a medium-sized force transmission framework, and investigation of versatile SOC recuperation approach is proposed to recoup adaptable battery SOC without influencing SOC limit for network occasion and guarantee

accessibility of BESS energy for the following conceivable aggravation occasion. To assess the BESS proficiency. Based on the results of the experiments, we suggest a BESS installation site with optimal BESS converter measurement for all the possible outcomes.

II. FREQUENCY STABILITY REQUIREMENTS

The similarity of matrix codes necessitates sufficient damping capacity, which may be achieved by readily available headroom to increase the output of generators or through remotely inserted energy storage devices. Dependable dynamic catalyst (up to its maximum age limit) for under-recurrence events and decreased dynamic force (hang type) for over-recurrence events are expected from the producing units. Depending on factors like country, fuel type (conventional or sustainable), and available options, the frequency of servicing is different. In this analysis, the baseline for evaluating network performance under the anticipated scenario events is the working guidelines by the Australian NEM. No matter what, the matrix must remain inside the non-basic recurring dead band of 0.997-1.003pu. The mandatory transient recurrence limit for age or burden events, according to NEM, is 0.99-1.01pu for 15 seconds and 0.997-1.003pu within 5 minutes. On the other hand, for network events, the cutoff is 0.98-1.02pu for 15 seconds, 0.99-1.01pu within 1 moment, and 0.9-1.1pu for voltage in the non-basic area within 5 minutes. In order to guarantee code consistency across frameworks, the aforementioned frequency requirements serve as a reference for setup, identify suitable BESS area and converter estimation, and provide the necessary force swaying damping.

III. CONTROL METHOD

A. Primary frequency control and RES

To keep up ostensible framework recurrence (inside non-basic recurrence working district), generator should coordinate the heap request continually by repaying any impermanent force bungles utilizing generator's put away dynamic energy. Along these lines, recurrence reaction by the lead representative for n framework can be characterized as in (1):

$$\frac{df}{dt} = \frac{fref}{2\sum Hn}\Delta Pd \qquad (1)$$

Where, $\Delta Pd = PG - PL, \Delta Pd1$ is the adjustment in power request, PG is the produced

ISSN: 1832-5505
Vol-7 Issue-02 MAY 2019

the heap power request, and its symbol is PL.∑ The total framework inactivity for all pivoting machines is denoted by **b***n*, and the apparent recurrence is denoted as $faef$. Overall latency is going lowered as a result of the fossil fuel power plants being turned down and the increasing entry of zero-inertial PV. Therefore, without improving framework inactivity through elective cycles, traditional lead representative controlled recurrence control may not effectively repay power irregular characteristics caused by aggravating events, such as changing PV yield, organisation, or burden possibility. Hence, as shown in Fig. 1, this study introduces an additional lead-slack regulated BESS to mitigate the antagonistic impact of PV penetration in the matrix, increase framework idleness steadiness, and aid in crucial recurrence management. With consolidated BESS, the recurrent response to manage uneven characters may be built as shown in (2):

$$\frac{df}{dt} = \frac{fref}{Hbess + 2\sum Hn}\Delta Pd \qquad (2)$$

Where, $Hbess$ is BESS dormancy steady, D1 and D2 are the hang coefficient of ageframework SG1 and SG2 separately.

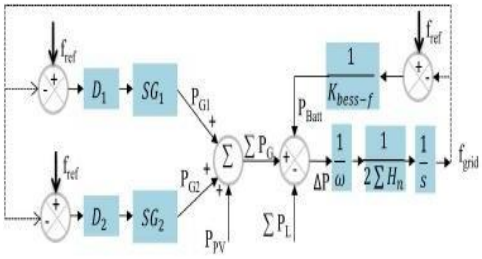

Fig.1. Primary frequency control with BESS The itemized model of the coordinated generatorsand BESS are examined and in Section III-B,separately.

B. The Overall Design of BESS and SOC Calculation

[6] A battery bank, a bidirectional force transformation framework, and a reasonably sized transformer for network connection are all shown in Fig. 2 as the overall BESS outline. Regulators for recurrence, voltage, dynamic/responsive (PQ), and charge make up the BESS converter control signals. By comparing the input reference signal with the operational constraints of the battery state of charge, the BESS converter is able to function as intended. All the detailed framework pieces of BESS, including the battery model, are presented throughout Sections III-B to III-E, and the point-by-point models of BESS are used to achieve recreation results.

[1] b

Here, Ibatt stands for the current through the battery, Cbatt for the apparent maximum current through the battery in ampere-hours (Ah), and _ for the Coulomb efficacy. In powerful simulations, it is reasonable to assume that the efficiency of the battery may change over the charging and discharging cycles, and thus the lossless inverter's claimed accuracy may be off. Regardless, several distributed exploration studies have taken zero inverter errors into

Fig. 2. Primary frequency control with BESS

The SOC figuring can be characterized by Coulomb including technique as (3)

$$SOC_t = SOC_{t-1} + \int^{t} \frac{\eta\, Ibatt}{3600\, Cbatt}\, dt \qquad (3)$$

account, such as setting charging and releasing efficiency to 100% for SOC error exams and dynamic investigations. The authors have decided to use a Coulomb efficiency estimate of 100% in this study due to the aforementioned setup works. Measured as the ratio of current to estimated battery limit, state-of-health (SOH) is a measure of how well a battery is holding its charge as it ages. The state of health (SOH) of an alternative battery is 100% and decreases when the battery is used for an hour. The difference between the Ah limit and SOC is used to establish the current battery limit. Nevertheless, SOH assessment isn't the main focus of our inquiry, thus interested readers are encouraged to read papers that include crucial data on SOH evaluation. Voltage at the battery's DC terminals is 0.9 kV, while voltage at the BESS AC side is 0.4 kV. The BESS AC side may be connected to the framework at different organisation voltages thanks to a 0.4/230kV advance up transformer. At its maximum charge, each battery has a voltage of 13.85V.

in addition to the 65 battery cells linked together. Developing an accurate model that captures the intricate electrochemical and nonlinear characteristics of a battery is an ambitious undertaking. However, there have been previous attempts to design a similar circuit, a Rint circuit with fewer limits and reasonable ease, to evaluate battery response. See Figure 3 for a square graph of the Rint identical battery model used in dynamic experiments.

Applied GIS

ISSN: 1832-5505
Vol-7 Issue-02 MAY 2019

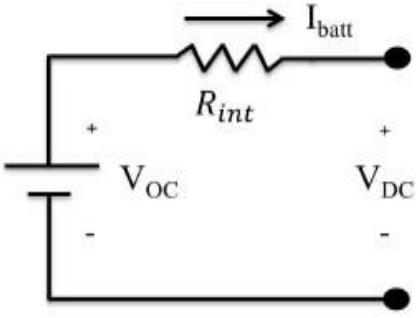

Fig.3. Block diagram of Rint equivalent battery model

The battery is planned as a voltage source that relies upon SOC with inside yield opposition (Rint) which can be assessed as in (4):

$$Vdc = V_{max}SOC + V_{min}(1 - SOC) - Ibatt\ Rint \quad (4)$$

A. BESS Damping Controller with Feedback Signals

Generous damping support is needed to successfully limit power framework motions in case of surprising transient occasions. The control circle that creates vital reference signals for BESSto contribute in damping control is appeared in Figs. 4 and 5. Since wide territory estimation isn't utilized, the neighborhood estimations for voltage and recurrence are utilized as contribution to control dynamic and responsive intensity of BESS.

1) Frequency droop controller:

The power frequency droop is enormously influenced with decreased framework latency and accordingly impact altogether on power frameworksteadiness. The fundamental idea of the embraced hang control is appeared in Fig. 6 and the ordinary hang qualities can be composed as in (5):

$$dpref = \frac{1}{Kbess - f}(fref - fgrid) \quad (5)$$

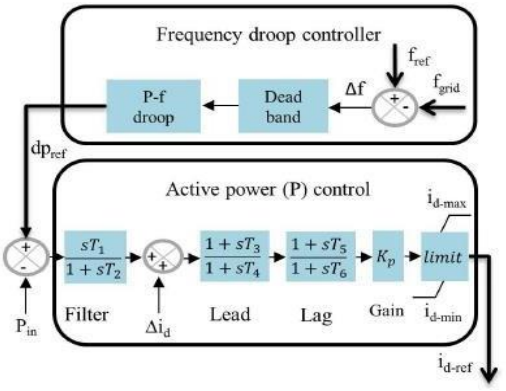

Fig. 4. The block diagram of frequency and BESS active power control

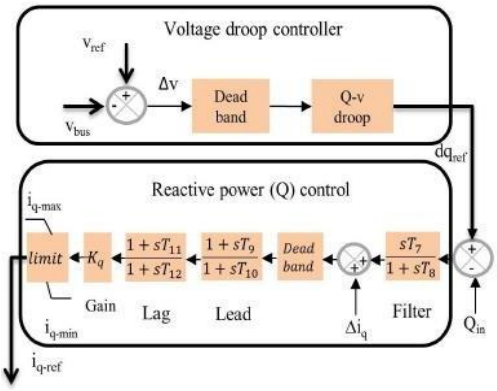

Fig. 5. The block diagram of voltage and BESS reactive power control

Where, $Fref$ is the recurrence reference (1pu), $dpref$ is the dynamic force referencedependent on power-recurrence (P-f) droop regulator, $Kbess - f$ is the hang boundary with the slant of $\frac{1}{Kbess-f}$BESS hang attributes (charging/releasing) can be exhibited in three working districts as appeared in Fig. 6. The battery stockpiling ought to expend surplus energy (charging mode) if real lattice recurrence $Fgrid >$ fch (charging recurrence), and conveys (releasing mode) power lack when $Fgrid <$ fch (releasing recurrence) as per their hang qualities. BESS can take an interest in an energy trade if battery SOC is accessible inside the characterized SOC requirements. The locale between fch (1.003pu) and $fdisch$ (0.997) is known as non-basic district as per Australian NEM recurrence working norm (dead band) that characterizes BESS inert area. Themost extreme charge power (P_{ch-max}) is actuated ($if\ fgrid > fch$) for a recurrence deviation of Δf_{max} long as SOC remains lower than greatest SOC as appeared in Fig. 6.

ISSN: 1832-5505
Vol-7 Issue-02 MAY 2019

The greatest release power ($P_{disch-max}$) is

Applied GIS

ISSN: 1832-5505
Vol-7 Issue-02 MAY 2019

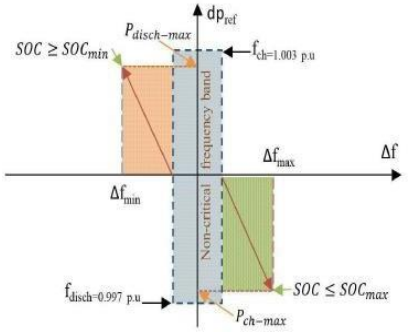

Fig. 6. Frequency droop characteristics

2) Voltage droop controller:

The standard of voltage droop regulator works along these lines as in recurrence hang regulatorand can be gotten as in (6):

$$d_{qref} = \frac{1}{K_{bess-v}} (V_{ref} - V_{grid}) \quad (6)$$

where, V_{ref} is the voltage reference (steady state voltage in pu), d_{qref} is the reactive power reference based on reactive power-voltage (Q-V) droop controller, K_{bess-v} is the voltage droop parameter whose slope is $\frac{1}{K_{bess-v}}$ BESS supports reactive power for positive and consumes reactive power for negative d_{qref} as shown in Fig. 7. The non-critical region (dead band) for voltage control is selected as 0.008pu, with a slope value of 10. The maximum reactive power supply Q_{max} is activated $(if\ V_{grid} < V_{supply})$ for a voltage deviation of as long as battery converter capacity is available. The maximum reactive power consumption $(-Q_{max})$ is activated $(if\ V_{grid} < V_{Consume})$ for a voltage deviation of ΔV_{max} until battery converter capacity reaches to its maximum limit.

3) Active / Reactive Power (PQ) Controller with Lead lag Controller:

Receptive force reference is generated by related responsive force estimations in q pivot and Δi_q from charge regulator, while dynamic force reference is created by the blunder between dynamic force yield at BESS AC terminal and force reference from recurrence hang regulator in d hub and Δi_d from charge regulator. The dynamic force reference signal is created using a lead-slack regulator and a first-request channel. In order to provide crucial separation and stage move, the PQ regulator uses a lead-slack sort stage compensator. Slack regulators have their posts closer to the starting point than their zeros, while lead regulators have their zeros closer to the beginning than the shafts.

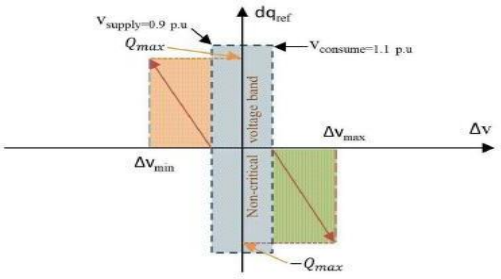

Fig. 7. Voltage droop characteristics

A lead-slack controller joins the upsides of individual controller to offer some motivation remembered execution for structure dauntlessness by diminishing reliable state error and settling time. The limiter in lead-slack controller portrays the constraint of force reference which is normally inside the best furthest reaches of BESS converter rating. The regular frameworks of shafts/zeros setting are discussed in [38], [39]. The trade limits with decided shafts/zeros regions of lead-slack controller to make dynamic power reference can be made as in (7):

$$K_d(s) = \frac{T_3\,(s+z_1)}{T_4\,(s+p_1)} \frac{T_5\,(s+z_2)}{T_6\,(s+p_2)} \quad (7)$$

The exchange capacities with determined shaft/zero areas of lead-slack regulator to create receptive force reference can be characterized as in (8):

$$K_q(s) = \frac{T_9\,(s+z_3)}{T_{10}\,(s+p_3)} \frac{T_{11}\,(s+z_4)}{T_{12}\,(s+p_4)} \quad (8)$$

Where, $T > T$, $T > T$ for lead controller and three, four, nine, ten} For the lag controller, $T5$ is greater than $T6$, and $T11$ is more than $T12$. The related parameters are $T3 = T9 = 40$, $T10 = 38$, $T5 = T11 = 13$, $T5 = T11 = 13$, $T6 = T12 = 35$, $z1 = z3 = 0.025$, $P1 = P2 = 0.026$, $Z2 = Z4 = 0.077$, $P2 = P4 = 0.028$, $Kp = 2.1$, $Kq = 0.1$, $T1 = T2 = T7 = T8 = 5$

B. Control of BESS and Management of Battery Charge and Discharge

BESS provides tremor dampening by absorbing surplus and supplying energy deficit during transient movements to alleviate temporary force shortage. For instance, the BESS inactive window exhibits the noncritical recurrence boundary Δ_f=±150mHz in Figure 6, which is necessary for controlling recurrences. In order to conserve power and improve power system security, a 50Hz (1pu) framework activates full BESS power for a 0.2Hz (0.004pu) frequency variation. This reduces age request lopsided features. As shown in (3), P-f hang characteristics directly affect upon the available fundamental force. The BESS current streams

ISSN: 1832-5505
Vol-7 Issue-02 MAY 2019

in the opposite direction of the recurrence change when the recurrence goes beyond the dead band window. The state of charge (SOC) of a battery, as shown in Figure 8, limits its ability to be charged or released. Unlike with

This study proposes a two-level flexible charging state of charge (SOC) method, which combines the conventional hang-type charging highest SOC with an additional flexible charging state of charge (SOC) edge, as an alternative to the current single-level SOC max/min breaking point for maintaining battery SOC [19]. In the proposed two-level (SOCmax or versatile SOC) flexible charging methodology, the main advantage is that any energising SOC cutoff can be selected by simply adjusting the benefit of charging current. This provides an additional level of charging flexibility according to the flexible scheduling of the BESS administrator for battery recharging.

1. BESS with Droop-type Charging/Discharging:

Without extra charging system, old style BESS charging/releasing is directed consequently as per the P-f hang qualities. BESS is intended to flexibly dynamic force, if battery SOC is more noteworthy than or equivalent to the base SOC for example 0.2pu and assimilate dynamic force, if SOC is not exactly or equivalent to the greatest SOC for example 1 for each unit. Thusly, in

general hang type charging/releasing procedure canbe characterized as in (9)

$$i_{d-in} = \begin{cases} i_{d-ref} & SOC \geq Soc_{min} \\ -i_{d-ref} & SOC \leq Soc_{max} \\ otherwise & \end{cases} \quad (9)$$

The greatest current count of the converter is determined as in (8) and (9):

$$i_{d-ref-out} = \int_{-|\max Value|}^{|\max Value|} i_{d-in}\, dt \quad (10)$$

$$i_{q-ref-out} = \int_{-y\ value}^{y\ value} i_{q-in}\, dt \quad (11)$$

$$y\ value = \sqrt{\left|\int_{0}^{|\max Value|^2 - i_{d-in}^2}\right|}$$

Where, and max= max Value=1. BESS hang type charging/releasing as indicated by the P-f qualities has critical control on the accessibility of fundamental battery limit. At post shortcoming harmony point, contingent upon the degree of dynamic force trades, SOC of the battery will change (decline/increment). Also, because of restricted productivity, battery self-releases over the idle time frame. This requires over-estimating the limit of BESS to abstain from arriving at least SOC and thus expands costs that decrease framework

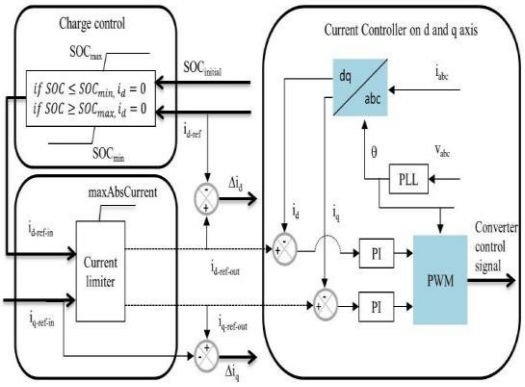

Fig. 8. The block diagram of BESS charge controller, d and q axis current control

This guarantees that sufficient BESS limit is accessible to partake in the following conceivable possibility occasion. The trading rationale of SOC can be composed as in (13) The received energizing system can be characterized as in (12)

i_{d-in}

$$(SOC_{min} + SOC_{max})$$

$$= \begin{cases} i_{ch-cur} & if\ SOC \leq \\ SOC \leq SOC & \\ min & \end{cases} \quad \begin{matrix} \\ and\ i_{d-ref}^{\ 2} < 0.0001 \end{matrix} \quad \begin{matrix} \\ or \end{matrix} \quad (12)$$

$$0 \quad otherwise$$

Where, i_{ch-cur} is the charging current when dynamic current reference on d hub is under 0.0001pu and SOC is lower than 0.5 or at SOCmin. Essentially, BESS current reference doesn't settle down to zero totally because of converter misfortunes and battery self-release and so on. Accordingly, reviving current is intended to act when dynamic current reference is under 0.0001pu. The energizing current of 0.01pu streams before battery scopes to the most extreme SOC 3) BESS gainfulness.

2) BESS Charging with Maximum SOC: On the off chance that SOC diminishes lower thana specific cutoff (may not be at least SOC), the goalaims to restore the state of charge (SOC) of the battery to its maximum possible level, which is 1 Pu, with minimal energy current consumption in the non-basic recurrence region or when the dynamic force reference current is very small.

Charging using Adaptive State of Charge: When the battery is fully charged, BESS cannot participate in any

ISSN: 1832-5505
Vol-7 Issue-02 MAY 2019

over-recurrence event that consumes excess power. Therefore, to regulate the BESS energy level within the administrators' defined window and preserve some recurrence edge for over recurrence events without affecting old style hang type charging/releasing or the most extreme SOC roof, an alternative point of control (SOC) limit for flexible charging is recommended. The first stage of battery charging while accused of versatile SOC is same to that of BESS Charging with Maximum SOC. The versatile state of charge limit is controlled by the charging current benefit. If the charging current is greater than the SOC exchanging edge, the SOC limitation will shift to the flexible SOC limit, which is defined by the BESS administrator. Here is a possible formulation of the SOC trading rationale: (13)

$$Soc_{adaptive} = \begin{cases} Soc_{max} & if\ i_{rch-cur} > i_{ch-threshold} \\ \max SOC & if\ i_{rch-cur} \leq i_{ch-threshold} \end{cases} \quad (13)$$

The selected value i_{ch-cur} threshold is0.1pu. Thusly, a reviving current of 0-0.1pu

ISSN: 1832-5505
Vol-7 Issue-02 MAY 2019

indicates a maximum SOC of 1 Pu. The estimated value of SOC versatile is 0.8pu, while the selected energising current $irch-cfr$ is 0.015pu. The BESS administrator may arrange for a balanced charging edge and charging current.
B. The Controller on the D and Q Axis at the Moment
In the d and q pivot, the current regulator reference is achieved by the BESS damping regulator, and the contributions to the current regulator are the purposeful d and q hub current signs of the converter's AC. Using a stage bolted circle (PLL) as a reference point and the same reference for the direct DC/AC converter, the current regulator adjusts the beat width balancing PMD and PMQ yield.

..

IV. Fuzzy logic controller:

The fuzzy rationale regulator is heavily dependent on the rules based. What matters is the data type and the results. Features like as mistake worth and change in blunder esteem are part of the fluffy logic regulator input.

Information values and rule designs are the foundation of the yield value. Variable restrictions ranging from -1 to 1. Factors could be either 0 or 1 in the reality assessment of Boolean logic.

Various types of fuzzy logic regulators have been identified, including fuzzification, rule networks, and defuzzification. The connections between the three regulators are shown in the circuit diagram below.

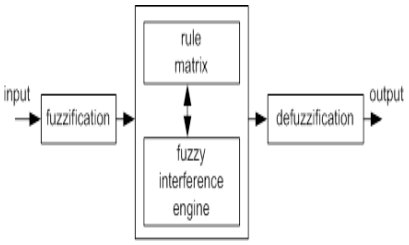

Fig.9. Fuzzy logic analysis and control

Fluffy principles are ordered relies on information and yield enrollment capacities. The schematic circuit graph of participation capacities demonstrated as follows

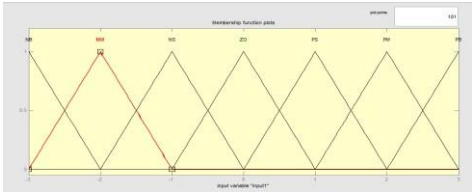

Fig.10. input-1 membership function

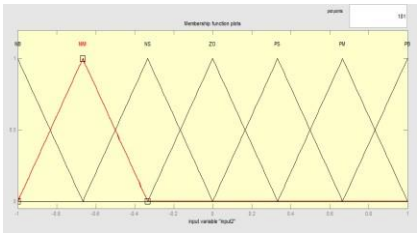

Fig.11. Input-2 membership function

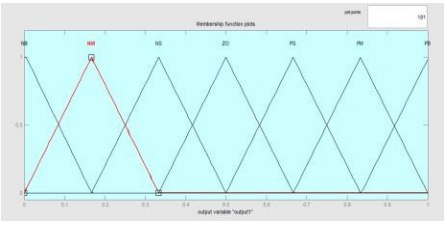

Fig.12. output membership function

e/Ce	NB	NM	NS	ZO	PS	PM	PB
NB	NB	NB	NB	NB	NM	NS	ZO
NM	NB	NB	NB	NM	NS	ZO	PS
NS	NB	NB	NM	NS	ZO	PS	PM
ZO	NB	NM	NS	ZO	PS	PM	PB
PS	NM	NS	ZO	PS	PM	PB	PB
PM	NS	ZO	PS	PM	PB	PB	PB
PB	ZO	PS	PM	PB	PB	PB	PB

Table:-1 Rules of fuzzy logic controller

In the fluffy rationale regulator input estimations of mistake and change in blunder and the yield. The standards are blend of 5 trianglecapacities and 2trapezoidal for each. The fundamental graph of info and yield participation capacities appeared in fig 10, fig 11, fig 12. These fluffy sets are interfaced by 'negative enormous (NB)','negative little (NS)', 'negative medium (NM)', 'positive huge (PB)', 'Zero (Z)', and 'Positivelittle (PS)','positive medium (PM)' for each fluffy enrollment capacities. The fluffy principles are directional by 49 for the five elements of mistake and change in blunder (Contribution of the FLC)

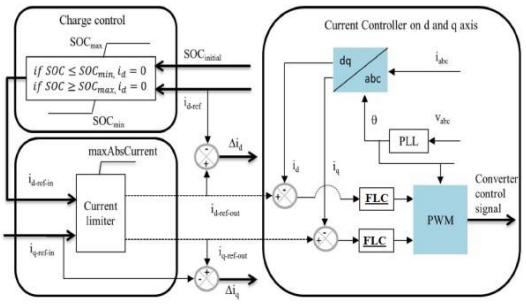

Fig.13. The block diagram of BESS charge controller, d and q axis current control using fuzzy logic controller

V. ATTRIBUTES OF THE TEST SYSTEM

ISSN: 1832-5505
Vol-7 Issue-02 MAY 2019

Figure 14 displays the results of studies on the impact of PV penetration on working recurrence using the IEEE 9-transport architecture. The reference machine in the dynamic model of generators is SG1 (hydro), and other models such as SG2 (gas turbine), SG3 (coal plant), and the organisation displaying nuances are available. As standard equipment, the generators come with an AVR and a lead representative. Connected to the organisation by a 0.6/230kV advance up transformer at transport 9, the collected PV is available with the accompanying data of itemised PV showing. Connected to the organisation at transport 7 using a 0.4/230kV advance up transformer, the BESS AC side voltage rating is 0.4kV. In order to shut down fossil fuel power facilities, the collected PV framework is taking sustainable energy into account and replacing the present coal-based SG3 unit. The purpose of implementing BESS is to meet the requirements of the lattice by providing more dampening and improving transient responses. "Case studies"

To investigate PV infiltration influence, two types of generator operating practices are taken into account. Method 1 in Table I describes a 100MW PV entry with apparent synchronised generator activity. Method 2 reflects the situation where selecting an advantageous generator yield option isn't possible to meet increased burden needs by adding the yields of the two generators, which is necessary due to ongoing burden development. In order to have a better understanding of the many aspects of efficiency issues caused by PV entry and to demonstrate the suggested SOC recovery technique, four examples are examined, two with and one without BESS: _

Case A: Line outage event with-
(a) Operating strategy 1
(b) Operating strategy 2
Case B: Load event with Operating strategy 1
Case C: BESS installation location and Converter sizing
(a) Operating strategy 2 for line loss
(b) Operating strategy 1 for load event
Case D: Battery recharging with Operating strategy 1
Case E: The operational flexibility and comparative advantages of the proposed adaptive SOC recovery

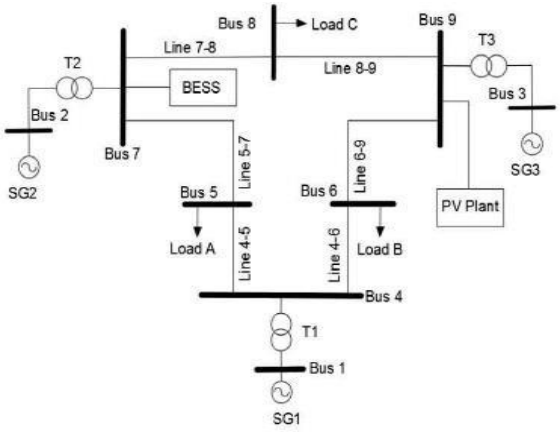

Fig. 14. The IEEE 9-bus system with PV and BESS location

TABLE I
ACTIVE POWER OF GENERATORS AND LOADS IN MW WITH DIFFERENT GENERATOR OPERATING STRATEGIES

Strategy	SG1	SG2	PV	Load A	Load B	Load c
Strategy 1	86	140	100	125	90	100
Strategy 2	107	165	100	150	110	100

Table.2. strategies with load and generator values

a. Simulation results using PI controller: Case-A:

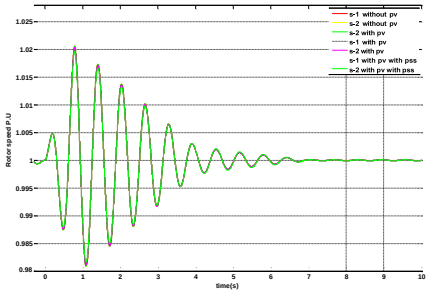

Fig.15. the frequency (Pu) oscillations of generator G2

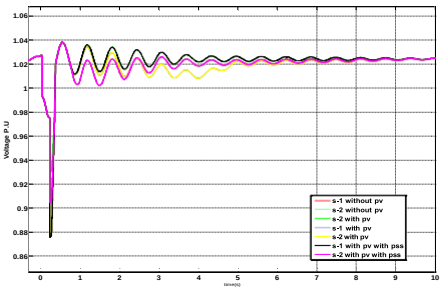

Fig16. Voltage at BESS connection point

ISSN: 1832-5505
Vol-7 Issue-02 MAY 2019

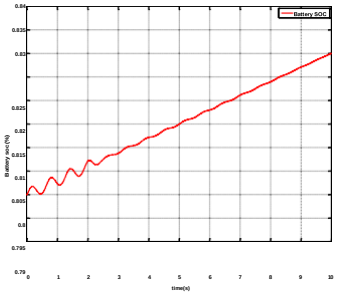

Fig17. Battery SOC

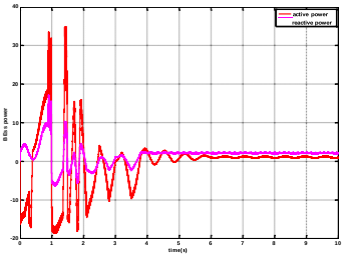

Fig18. The active and reactive power of BESS

Case-B

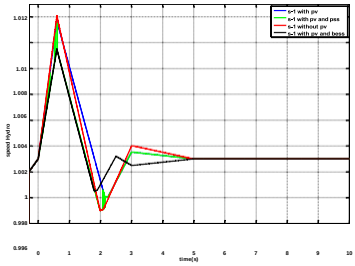

Fig19. The frequency (pu) oscillation of generator G1 with load event

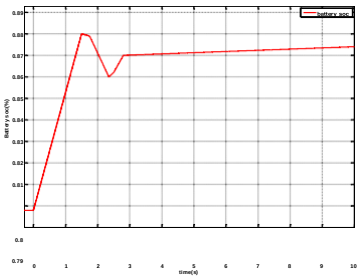

Fig20. Battery SOC

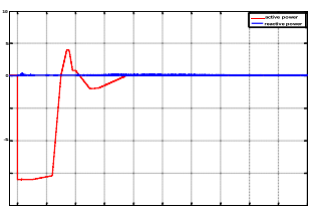

BESS Installation Location and Converter Sizing - Case C:

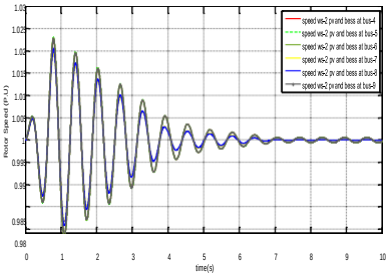

A

Fig.22. Generator frequency with BESS installed at different buses:

Case D:

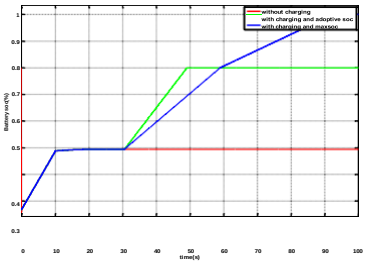

A.

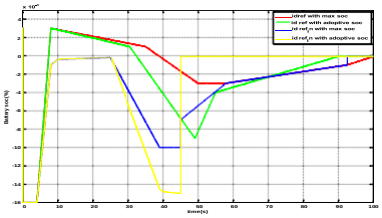

B

Fig23. SOC status with different charging mechanism

Case-E:

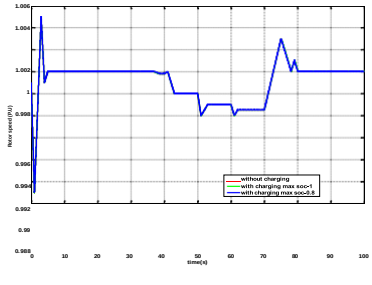

ISSN: 1832-5505
Vol-7 Issue-02 MAY 2019

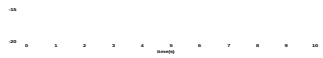

Fig21. The active and reactive power of BESS

A

Fig24. The frequency of generators [p.u.] and voltage oscillations [p.u.] at bus and PCC with BESS

ISSN: 1832-5505
Vol-7 Issue-02 MAY 2019

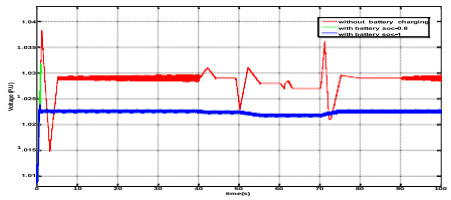

A

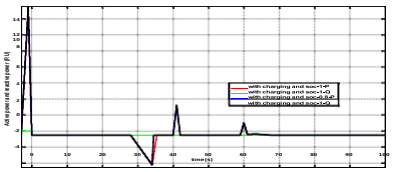

B

Fig25. Voltage at BESS connection point (a) BESS active/reactive power (b)

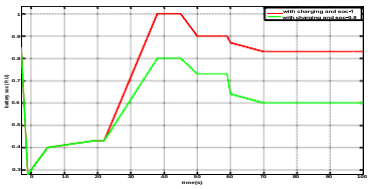

Fig26. SOC status with different charging mechanism

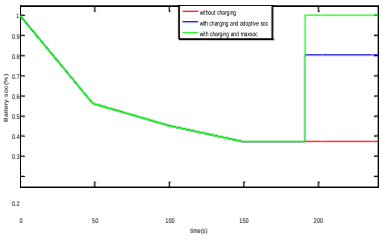

Fig27. SOC status with different charging mechanism

b. Simulation results using fuzzy logic controller:

Case-A

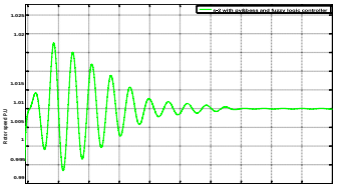

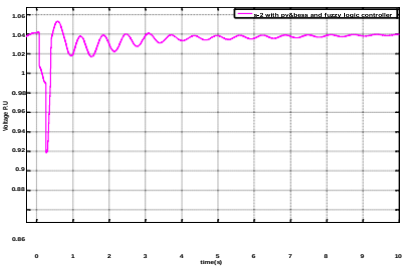

Fig.29. Voltage at BESS connection point

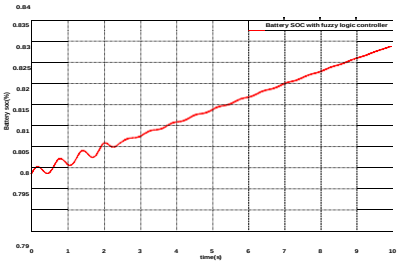

A

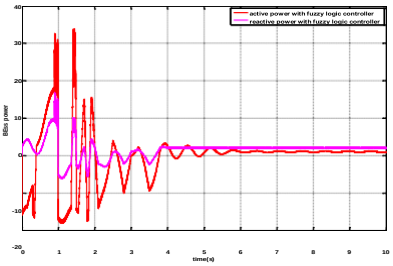

B

Fig30. battery SOC (a) The active and reactive power of BESS (b)

Case-B

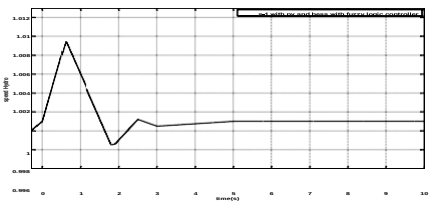

Fig.31. The frequency (pu) oscillation of generator G1 with load event

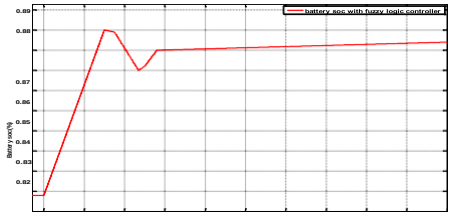

ISSN: 1832-5505
Vol-7 Issue-02 MAY 2019

Fig.28. The frequency (pu) oscillations of generator G2

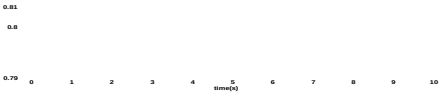

Fig.32. battery SOC

ISSN: 1832-5505
Vol-7 Issue-02 MAY 2019

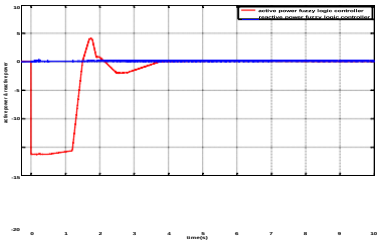

Fig33. The active and reactive power of BESS

Case-C

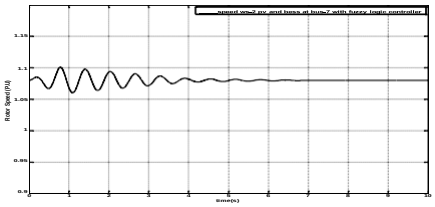

Fig.34. Generator frequency with BESS installed at different buses:

CaseD:

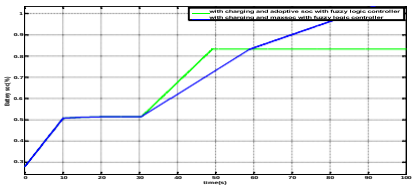

a

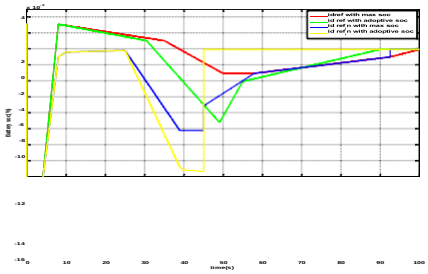

b

fig35. SOC status with different charging mechanism

Case-E

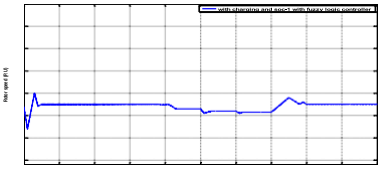

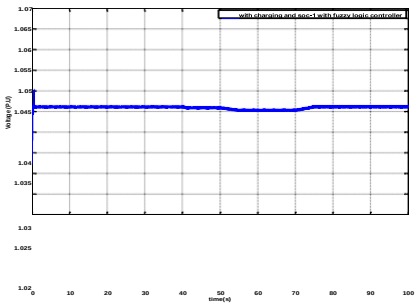

Fig37. Voltage at BESS connection point (a)

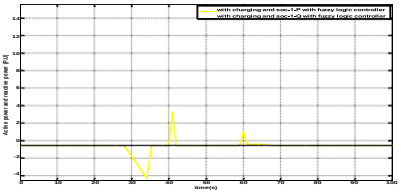

Fig.38 BESS active/reactive power

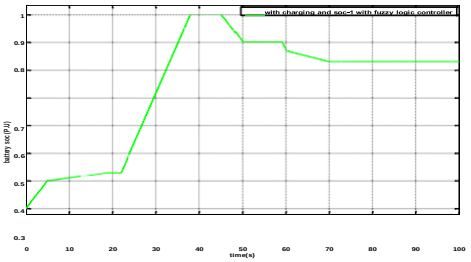

Fig39. SOC status with different charging mechanism

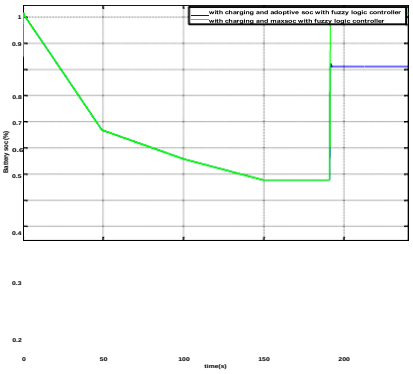

Fig40. SOC status with different charging mechanism

ISSN: 1832-5505
Vol-7 Issue-02 MAY 2019

VI. CONCLUSION

Extra damping and improved vital recurrence response with increased PV entry level in the force framework are offered by a hang type, lead-slack controlled BESS with unique SOC recovery approach and fluffy reasoning regulator. Improved flexibility is provided by the flexible SOC recovery method.

Figure 36 shows the voltage oscillations at the bus and PCC with BESS, as well as the frequency of the generators (p.u.).

Instead of using the outdated hang type charge for future temporary events, BESS energy executives are planning based on PV figures. Considerations of reproduction reveal that, according to NEM models, the framework's responses to abuse

guidelines for matrix recurrence with and without a PSS when PV entry increases. However, by providing additional framework dampening, integrating BESS effectively regulates and reduces system movements. As a result, it's clear that BESS can mitigate PV's latency-related drawbacks, comply with lattice standards, and avoid penalties for violating those standards. The suggested flexible SOC recovery allows for the acquisition of a variable resurrecting SOC level according to the BESS administrator's plan and PV/other estimation, and it does not limit itself in the event of an unexpected organisational event. The added benefit of flexible operating arrangement of BESS may be achieved at any time thanks to this. Improving system performance by increasing PV entry level, their impact on transient recurrence stability, and novel BESS control algorithms.

VII. REFERENCES

1. International Energy Agency, “Renewables 2017, [Available Online]: https://www.iea.org/publications/renewables2017, [Accessed on: 2018- 07-01].”
2. P. Du and Y. Makarov, “Using disturbance data to monitor primary frequency response for power system interconnections,” IEEE Transactions onPower Systems, vol. 29, no. 3, pp. 1431– 1432, May 2014.
3. S. Eftekharnejad, V. Vittal, G. T. Heydt, B. Keel, and J. Loehr, “Small signal stability assessment of power systems with increased penetration of photovoltaic generation: A case study,” IEEE Transactions on Sustainable Energy, vol. 4, no. 4, pp. 960–967, Oct 2013.
4. R. Shah, N. Mithulananthan, and R. Bansal, “Oscillatory stability analysis with high penetrations of large-scale photovoltaic generation,” Energy Conversion and

ISSN: 1832-5505
Vol-7 Issue-02 MAY 2019

Management, vol. 65, pp. 420 – 429, 2013, Global Conference on Renewable Energy and Energy Efficiency for Desert Regions 2011 GCREEDER 2011.

5. S. You, G. Kou, Y. Liu, X. Zhang, Y. Cui, M. J. Till, W. Yao, and Y. Liu, "Impact of high PV penetration on the inter-area oscillations in the u.s. eastern interconnection," IEEE Access, vol. 5, pp. 4361–4369, 2017.
6. R. Shah, N. Mithulananthan, and K. Y.Lee, "Large-scale PV plant with a robust controller considering power oscillation damping," IEEE Transactions on Energy Conversion, vol. 28, no. 1, pp. 106–116, Mar 2013.
7. D. Remon, A. M. Cantarellas, J. M. Mauricio, and P. Rodriguez, "Power system stability analysis under increasing penetration of photovoltaic power plants with synchronous power controllers," IET Renewable Power Generation, vol. 11, no.6, pp. 733–741, 2017.
8. D. Remon, C. A. Ca˜nizares, and P. Rodriguez, "Impact of 100-mw-scale PV plants with synchronous power controllers on power system stability in northern chile," IET Generation, Transmission Distribution, vol. 11, no. 11, pp. 2958–2964, 2017.
9. L. Zhou, X. Yu, B. Li, C. Zheng, J. Liu, Q. Liu, and K. Guo, "Damping inter-area oscillations with large-scale PV plant by modified multiplemodel adaptive control strategy," IEEE Transactions on Sustainable Energy, vol. 8, no. 4, pp. 1629–1636, Oct 2017.
10. H. Xin, Y. Liu, Z. Wang, D. Gan, and T. Yang, "A new frequency regulation strategy for photovoltaic systems without energy storage," IEEE Transactions on Sustainable Energy, vol. 4, no. 4, pp. 985–993, Oct 2013.
11. Z. Jietan, Q. Linan, R. Pestana, L. Fengkui, and Y. Libin, "Dynamic frequency support by photovoltaic generation with "synthetic" inertia and frequency droop control," in 2017 IEEE Conference on Energy Internet and Energy System Integration (EI2), Nov 2017, pp. 1–6.
12. V. A. K. Pappu, B. Chowdhury, and R. Bhatt, "Implementing frequency regulation capability in a solar photovoltaic power plant," in North American Power Symposium 2010, Sep 2010, pp. 1–6.